Complex domain nonlocal group-wise sparsity: toward wavelength super-resolution phase imaging in coherent optics

Vladimir Katkovnik and Karen Egiazarian
Signal Processing Laboratory, Tampere University of Technology, Tampere, Finland
Email: vladimir.katkovnik@tut.fi, karen.egiazarian@tut.fi

Phase imaging is one of the key instruments in optics allowing to make visible invisible features of specimens and produce precise measurements with resolution on the level of wavelengths (e.g. [1]- [3]). It is possible due to a phase sensitivity of coherent wavefront to shape and internal structure of specimens. While only intensity of light fields can be measured, visualization of phase from intensity observations is an important problem. In the phase contrast microscopy the wavefront modulation in the Fourier plane was developed to resolve this problem (Frits Zernike 1930s, Nobel prize 1953). Despite the revolutionary success of these methods only a *qualitative visualization* of phase can be achieved in this way, where features of specimens even visible maybe be so distorted that accurate measurements are not possible and even a proper interpretation can be problematic.

Quantitative visualization is targeted on direct phase imaging and precise measurements. Roughly speaking there are two ways to achieve this goal. The first one is off-axis *holography* with measurements given as intensities of sums of reference and object beams. The *phase retrieval* (or *in–line holography*) is an essential alternative because it does not require a reference beam.

In the modern development the quantitative phase imaging techniques are fundamentally based on digital data processing. Let us consider for instance the following formalization of the so-called phase retrieval problem:

$$z_s = |\mathcal{P}_s\{u_o\}|^2,\ s = 1, ..., L, \tag{1}$$

where: $u_o \in \mathbb{C}^{N\times N}$ is an $N\times N$ complex-valued object (specimen) 2D image; $\mathcal{P}_s$: $\mathbb{C}^{N\times N} \longmapsto \mathbb{C}^{M\times M}$ is a complex-valued operator of wavefront propagation from the object to sensor planes, $y_s \in \mathbb{R}_+^{M\times M}$ is an $M\times M$ intensity images of the wavefronts at the sensor plane.

In the setup with a thin lens shown in Fig. 1 the forward propagation operator $\mathcal{P}_s\{u_o\}$ linking the object and sensor wavefronts, u_o and u_s, is of the form

$$u_s(\xi,\eta) = \mu \exp\{j\frac{\pi}{\lambda f}(\xi^2+\eta^2)\}\mathcal{F}_{u_o\cdot\mathcal{M}_s}(\xi/\lambda f, \eta/\lambda f), \tag{2}$$

where $\mathcal{F}_{u_o\cdot\mathcal{M}}$ stands for the Fourier transform of the product $u_o(x,y)\mathcal{M}_s(x,y)$, $\mathcal{M}_s(x,y)$ is a complex valued transmission (or reflection) function of the phase modulation mask, λ is the wavelength and f is a focal length of the lens.

Reconstruction of the complex-valued object $u_o = a_o\exp(i\varphi_o)$ from noiseless or noisy observations $\{z_s\}$ is *phase retrieval problem*. Here *phase* emphasizes that in the object the phase is a variable of the first priority while the amplitude may be an auxiliary variable often useful only in order to improve phase imaging.

Sparsity for u_o can be imposed in the following different ways:

(1) Complex-valued u_o;

(2) Real-valued pair: phase φ and amplitude a_o;

(3) Real-valued pair: real and imaginary parts of u_o.

The phase retrieval for the considered problem provided Poissonian noisy observations is formalized as the Nash equilibrium balancing on $(\{\mathbf{u}_s\}_1^L, \mathbf{u}_o, \boldsymbol{\theta}_a, \boldsymbol{\theta}_\varphi)$ two criteria [4]:

$$\mathcal{L}_1(\{\mathbf{u}_s\},\mathbf{u}_o) = \sum_{s=1}^{L}\sum_{l=1}^{n}[|\mathbf{u}_s[l]|^2\chi - \mathbf{z}_s[l]\log(|\mathbf{u}_s[l]|^2\chi)] + \frac{1}{\gamma_1}\sum_{s=1}^{L}||\mathbf{u}_s - \mathcal{P}_s\{\mathbf{u}_o\}||_2^2,$$

$$\mathcal{L}_2(\boldsymbol{\theta}_\varphi,\boldsymbol{\theta}_a,\boldsymbol{\varphi},\mathbf{a}) = \tau_a\cdot||\boldsymbol{\theta}_a||_0 + \tau_\varphi\cdot||\boldsymbol{\theta}_\varphi||_0 + \frac{1}{2}||\boldsymbol{\theta}_a - \Phi_a\mathbf{a}||_2^2 + \frac{1}{2}||\boldsymbol{\theta}_\varphi - \Phi_\varphi\boldsymbol{\varphi}||_2^2,\ \mathbf{u}_o = \mathbf{a}\circ\exp(j\boldsymbol{\varphi}).$$

Here we use the sparsity in amplitude and phase variables, where analysis Φ_a and synthesis Φ_φ frames are designed using BM3D technique, i.e. nonlocal group-wise sparsity, and $\boldsymbol{\theta}_a$ and $\boldsymbol{\theta}_\varphi$ are the respective spectral variables for amplitude and phase.

It is shown for this formalization that the BM3D sparsity results in the separate filtering of phase and amplitude of the form:

$$\hat{\boldsymbol{\varphi}} = BM3D_{phase}(\boldsymbol{\varphi}_{,}, th_\varphi),$$
$$\hat{\mathbf{a}} = BM3D_{ampl}(a, th_B),$$

where BM3D stands for BM3D thresholding filtering.

Here *phase* and *ampl* as indices of BM3D are used in order to emphasize that the parameters of BM3D can be different for phase and amplitude.

BM3D procedures update (filter) input superindices variables; th_φ and th_B are threshold parameters of the algorithms.

This kind of phase/amplitude as well as real/imaginary parts sparsity modeling has been applied for a number of phase imaging problems (e.g. [5]-[8]). The complex domain sparsity targeted on direct sparse approximations of $\mathbf{u}_o$ appeared in the recent works [10]-[12].

The main contribution of this paper is a development of super-resolution phase retrieval for optical setup in Fig.1, where a random phase modulation is implemented by a spatial light modulators (SLM) located in the object plane. Some simulation examples (see Figs. 2-6) demonstrate results obtained for the sub-wavelength phase imaging provided that the computational pixels as small as $\lambda/4$, where λ is the wavelength of coherent wavefront. Note that in these examples the resolution factor with respect to the pixel size of the sensor and SLM (RF_S) is equal to 32.

Acknowledgment

This work is supported by Academy of Finland, project no. 287150, 2015-2019.

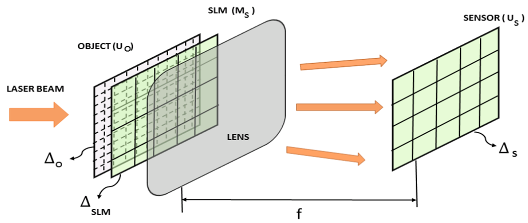

Fig. 1. Optical setup with a single lens for phase retrieval from modulated diffractive patterns: Object (o), Spatial light modulator (SLM), Lens and Sensor (s). The object is placed against the lens and the distance from the lens to the sensor is equal to the focal length of the lens f. The object, lens and spatial light modulator (SLM) shown between the object and lens are located in the same plane. In this consideration the object, SLM and lens are wavefront transformers for a uniform monochromatic normally incident plane wave (laser beam).

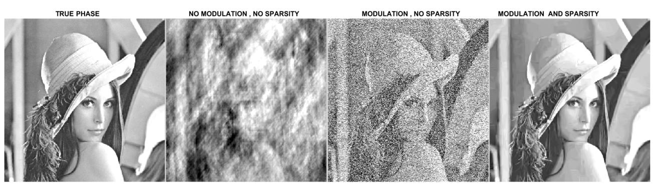

Fig. 2. Phase reconstructions from left-to-right: (a) true lena image, (b) reconstruction without phase modulation, (c) reconstruction with phase modulation but without SPAR filtering, (d) reconstruction with phase modulation and with SPAR filtering, $L = 1$, $RF = 1$, $\chi = 10000$.

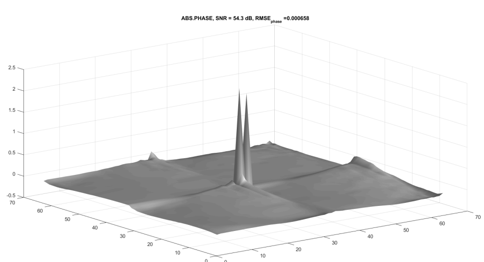

Fig. 3. 3D surfaces for sub-wavelength reconstruction of two phase picks images. The distance between the picks is equal to 0.257 λ .

References

[1] R. K. Tyson. *Principles of Adaptive Optics*. 4rd ed., CRC Press, 2014.

[2] Th. Kreis, *Handbook of Holographic Interferometry*. Wiley-VCH, Berlin, 2005.

[3] B. Kress and P. Meyrueis. *Applied Digital Optics: From Micro-Optics to Nanooptics*. John Wiley & Sons, Inc., 2009.

[4] V. Katkovnik, "Phase retrieval from noisy data based on sparse approximation of object phase and amplitude", submitted, http://www.cs.tut.fi/~lasip/DDT/pdfs/Single_column.pdf (2015).

[5] V. Katkovnik and J. Astola, " High-accuracy wavefield reconstruction: decoupled inverse imaging with sparse modeling of phase and amplitude," J. Opt. Soc. Am. A, vol. 29, (2012) 44 – 54.

[6] V. Katkovnik and J. Astola, "Compressive sensing computational ghost imaging," J. Opt. Soc. Am. A, vol. 29 no. 8 (2012) 1556-1567.

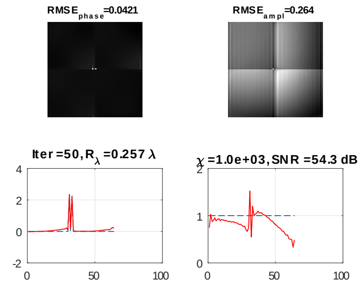

Fig. 4. Two-picks reconstructions, Distance between peaks 0.257 λ. Four 32 x 32 squares well seen in amplitude reconstructions correspond to four pixels of SLM. The cross-sections are shown for the middle horizontal line: solid ('red') for reconstructions and dotted ('blue') for true variables.

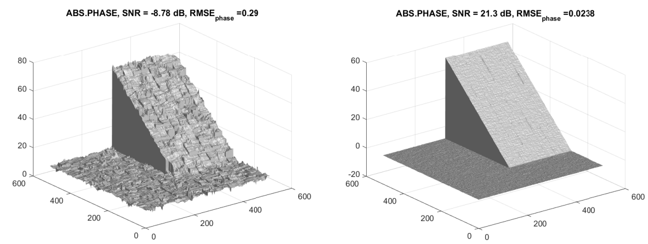

Fig. 5. Sub-wavelength resolution of share plane absolute phase, maximum value 56.8 rad. Reconstructions from the very noisy data χ=1 (left, failed) and the lowest noise level χ=1000 (right).

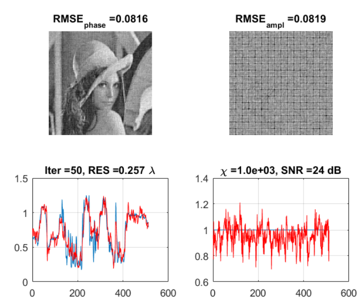

Fig. 6. Super-resolution SPAR Lena phase image reconstrctions, RF=32.

[7] V. Katkovnik and J. Astola, "Sparse ptychographical coherent diffractive imaging from noisy measurements," J. Opt. Soc. Am. A, vol. 30 (2013) 367-379.

[8] C. A. Metzler, A. Maleki, R. G. Baraniuk, "BM3D-PRGAMP: Compressive phase retrieval based on BM3D denoising," IEEE International Conference on Image Processing (ICIP), 2016.

[9] V. Katkovnik, "Phase retrieval from noisy data based on sparse approximation of object phase and amplitude", submitted, (2016) http://www.cs.tut.fi/~lasip/DDT/index3.html.

[10] H. Hongxing, J. M. Bioucas-Dias, and V. Katkovnik, "Interferometric phase image estimation via sparse coding in the complex domain," IEEE Trans. on Geoscience and Remote Sensing, vol. 53 no. 5 (2015) 2587 - 2602.

[11] V. Katkovnik, K Egiazarian, J. Bioucas-Dias,'Phase imaging via sparse coding in the complex domain based on high-order SVD and nonlocal BM3D techniques,' *Proceedings of IEEE International Conference on Image Processing* (*ICIP 2014*), (2014) 4587-4591.

[12] V. Katkovnik and K. Egiazarian, "Complex domain sparse phase imaging based on nonlocal BM3D techniques", (2016) http://www.cs.tut.fi/~lasip/DDT/index3.html.